

# Synergistic Interplay between Promoter Recognition and CBP/p300 Coactivator Recruitment by FOXO3a

Feng Wang<sup>†,\*</sup>, Christopher B. Marshall<sup>†,\*</sup>, Guang-Yao Li<sup>†,\*</sup>, Kazuo Yamamoto<sup>†,§</sup>, Tak W. Mak<sup>†,§</sup>, and Mitsuhiro Ikura<sup>†,\*,\*</sup>

<sup>†</sup>Department of Medical Biophysics, University of Toronto, Toronto, ON, Canada M5G 2M9, <sup>\*</sup>Division of Signaling Biology, Ontario Cancer Institute, University Health Network, Toronto, ON, Canada M5G 1L7, and <sup>§</sup>The Campbell Family Cancer Research Institute, University Health Network, and Department of Immunology, University of Toronto, Toronto, ON, Canada M5G 2C1

The forkhead box (FOX) protein family contains about 200 transcription factors (1) (details at <http://biology.pomona.edu/fox/>), which all contain a conserved forkhead (FH) DNA-binding domain, flanked by more divergent sequences (2, 3). These proteins, which serve diverse functions, have been divided into 19 subfamilies (FOXA to FOXS) based on phylogenetic analysis (4). The FOXO subfamily includes four members in mammals: FOXO1 (FKHR), FOXO3a (FKHRL1), FOXO4 (AFX), and FOXO6 (5). The genes encoding the first three proteins, which share high functional and sequence similarity, were identified in fusion genes from chromosomal translocations occurring in human rhabdomyosarcomas and acute myeloid leukemias (6–8), whereas the more distantly related FOXO6 was recently identified by degenerate PCR screening (9).

FOXO3a is ubiquitously expressed to varying levels in all tissues, with especially high expression in the adult brain (5). As a transcription factor, FOXO3a binds to a consensus DNA sequence (G/C/A) (T/C/A) AAA (T/C) A (10, 11), named forkhead response element (FRE), through the FH domain. It has been shown that the CREB-binding protein (CBP) and p300 are the coactivators of FOXO proteins, enhancing gene transcription by recruiting basal transcriptional machinery or remodeling chromatin structure through intrinsic histone acetyltransferase (HAT) activity (12). It was first shown that the *C. elegans* FOXO homologue, DAF-16, recruits CBP to activate gene transcription, and subsequently the physical interactions between human FOXO proteins and CBP were identified and mapped (13, 14). FOXO3a regulates the transcription of a variety of genes and is in-

**ABSTRACT** FOXO3a is a transcription factor belonging to the forkhead box O-Class (FOXO) subfamily, and it regulates metabolism, cell-cycle arrest, cell differentiation, and apoptosis through activating or suppressing gene transcription. FOXO3a contains a well-folded DNA-binding forkhead (FH) domain, but a large portion of the remaining protein sequence (75% of the total) is predicted to comprise intrinsically disordered regions (IDRs). Within the IDRs, there are three conserved regions (CR1–CR3), and it has been shown that CR3 (residues D610–N650) is a transactivation domain that recruits the coactivator histone acetyltransferase (HAT) CBP/p300, through binding to its KIX domain. In a previous study, we determined the solution structure of the FH domain and identified an intramolecular interaction between FH and CR3 domains of FOXO3a. Here we illustrate that the KIX domain of CBP interacts with the central core region (L620–A635) of CR3, which also internally interacts with the FH domain. In this heterotypic interplay, FH prevents CR3 from binding to KIX; however, upon binding to the Forkhead response element (FRE) DNA, the FH domain releases the CR3 domain, allowing it to interact with KIX. While previous studies have shown that the transactivation domains of c-Myb and MLL bind to distinct sites on KIX, our results indicate that FOXO3a CR3 has an ability to bind to both of these sites. These results suggest a model of FOXO3a-dependent coactivator recruitment in which the dynamic interplay between KIX and FH domains for binding to CR3 plays a key regulatory role in gene transcription activation.

\*Corresponding author,  
mikura@uhnres.utoronto.ca.

Received for review July 28, 2009  
and accepted October 12, 2009.

Published online October 12, 2009

10.1021/cb900190u CCC: \$40.75

© 2009 American Chemical Society



tor of cell survival versus death. In addition to its transcriptional activity, FOXO3a also interacts with numerous proteins, including p53, ATM, and  $\beta$ -catenin, to play a pivotal role in a complex signaling network (23–26).

With the increasing interest in the biological significance of FOXO, these proteins have been extensively studied and much effort has been made toward the structural characterization of FOXO proteins. However, most results are limited to the FH domain (24, 27–29) (Figure 1, panel a). Outside of the well-folded FH domain, which is conserved among all forkhead transcription factors, other parts of FOXO proteins are predicted to be intrinsically disordered (30). Among FOXO3a, FOXO1, and FOXO4, there are three conserved regions (CR1–CR3) located in the intrinsically disordered regions (IDRs). The CR3 domain is an acidic transactivation domain (Figure 1, panel a), which binds directly to the KIX domain of the transcription coactivator CBP (14, 31). The KIX domain mediates interactions with transactivation domains of many transcription factors, including CREB, p53, c-Myb, and MLL, and possesses two distinct hydrophobic grooves that can bind two transactivation domains simultaneously in a cooperative manner (32–36). In a previous study, we demonstrated that the CR3 domain is engaged in an intramolecular interaction with the FH domain, and NMR titration experiments revealed that the CR3-binding site partially overlaps with the DNA-binding site on the FH domain (Figure 1, panel b) (24, 28, 37).

Considering that the DNA-binding activity of the FH domain and the coactivator-recruitment activity of the CR3 domain are crucial for transcriptional activation, we sought to examine the role of the intramolecular interaction between these regions in coactivator recruitment. In this study, we demonstrate that the FH domain inhibits the binding of the CR3 domain to the KIX domain, but binding of FRE DNA to the FH domain releases the CR3 domain, promoting the recruitment of CBP to the transcriptional initiation site. We will discuss the role of this intramolecular interaction of FOXO3a in CBP-mediated transcriptional activation.

## RESULTS AND DISCUSSION

**FH and KIX Bind to the Same Region on CR3.** The CR3 domain of FOXO3a (D610–N650) is mainly unstructured in solution as shown by circular dichroism (CD) and NMR (24). However the central core region (D623–I628, and L632–D634) is predicted to be helical

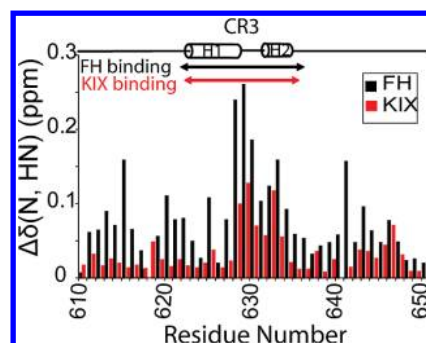


**Figure 2. Chemical shift perturbation of CR3 induced by FH and KIX.** The normalized backbone amide chemical shift changes in the CR3 HSQC peaks induced by FH (black) and KIX (red) were calculated using the equation  $\Delta\delta(\text{N, HN}) = \sqrt{[(\Delta\text{HN})^2 + (\Delta\text{N}/6.5)^2]}$  and plotted against the residue number. Secondary structure prediction of the CR3 domain is shown above, and the regions most affected by FH and KIX are indicated with black and red arrows (residues L620–A635).

(Figure 2) (30), and titration of the CR3 peptide with trifluoroethanol (TFE) induces helical secondary structure as demonstrated by far UV CD spectra (24). These data suggest that the CR3 domain has strong propensity to form helical structure in a hydrophobic environment. In our previous study, the central core region of the CR3 domain was found to bind to both FOXO3a FH domain (Supplementary Figure 1, panel a) and the DNA-binding domain (DBD) of p53 (24). The CR3 domain of FOXO3a has also been identified as the KIX-interacting site (14); however, detailed information is still elusive. To identify regions of the CR3 that are involved in interaction with KIX, we added unlabeled KIX to  $^{15}\text{N}$ -labeled CR3, recorded the HSQC spectra (Supplementary Figure 1, panel b), and calculated the normalized chemical shift changes for each backbone peak using the previously determined assignments (24). The results clearly show that the same region of the CR3 domain interacts with both FH and KIX (Figure 2). This central core region contains 5 negatively charged residues as well as 5 non-polar residues, which likely mediate protein–protein interaction through hydrophobic and electrostatic interactions, respectively.

**FH Domain Inhibits CR3 from Binding to the KIX Domain.** The finding that the FH domain of FOXO3a and the KIX domain of CBP bind to a common site in FOXO3a CR3 domain raises the question of how the intramolecular FH–CR3 interaction affects the ability of

CR3 to bind KIX and recruit the coactivator CBP. The FH domain and the CR3 domain are linked by a long putative IDR (V252–S609), which would be expected to enhance the binding affinity by increasing the encounter rate of two linked parts. Unfortunately, the unstructured region is vulnerable to protease digestion when expressed in *E. coli*. As an alternative approach, we engineered an FH-CR3 fusion (denoted FCF) protein in which the FH domain and CR3 domain are linked by four “Gly-Ser” repeats (Figure 3, panel b). The FCF exists in a closed state with FH bound to CR3, as shown by its  $^{15}\text{N}$ -HSQC spectrum (24).

First, we added unlabeled CR3 peptide to  $^{15}\text{N}$ -labeled KIX and observed significant chemical shift changes, indicating an interaction between FOXO3a CR3 domain and the KIX domain of CBP (Figure 3, panel a). However, when FCF was added to the  $^{15}\text{N}$ -labeled KIX domain, fewer peaks were perturbed and chemical shift changes were much smaller in magnitude relative to the addition of CR3 domain alone (Figure 3, panels a and b), indicating that the FH domain inhibits the binding of the CR3 domain to the KIX domain. To confirm that this observation is not an artifact caused by the short linker in the FCF protein, we performed pull-down experiments with *in vitro* translated FOXO3a fragments with the natural sequence (Figure 3, panel c). A construct (S151-G673) containing both intact FH and CR3 domains bound to the KIX domain much more weakly than a construct (G244-G673) in which the CR3-binding site in the N-terminus of the FH domain was truncated (Figure 3, panel c). Therefore the FH domain decreases the affinity of the CR3 for the KIX domain of CBP, and binding is recovered by deletion of FH. The results are consistent with the NMR data using the FCF protein.

**FRE DNA Displaces CR3 from the FH Domain.** For efficient FOXO3a-dependent transcription initiation, the inhibitory effect of the FH-CR3 intramolecular interaction must be counteracted. We propose that the FRE consensus DNA sequence found in the promoter region of FOXO3a-regulated genes is a crucial player in this process. We have shown by NMR titration that the CR3 binds to a hydrophobic cleft composed of the N-terminal loop, H1, H3, and H4 (Figure 1, panel b) (24), while the crystal structure of FOXO3a-DNA complex and some biochemical studies show that the DNA-binding surface of FH domain is composed of the N-terminal loop, H3, the C-terminal loop, and the loop between S2 and S3 (called Wing1) (Figure 1, panel b) (28, 37). Thus the CR3-

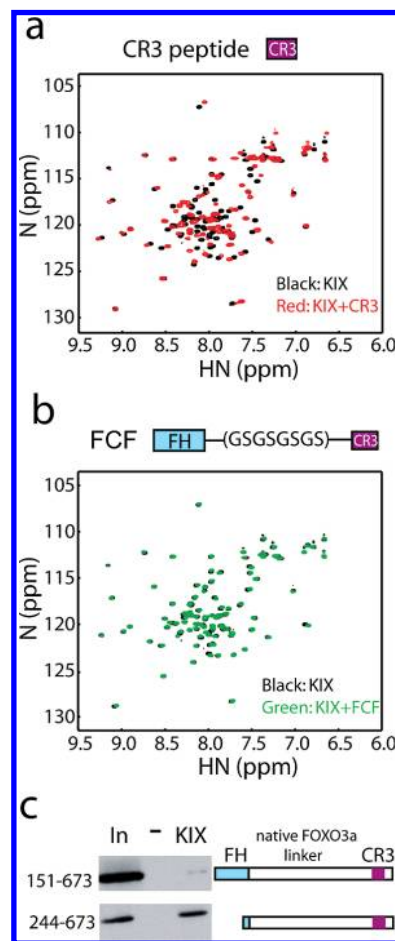


**Figure 3. FH domain inhibits CR3-KIX interaction.** a) Overlaid  $^1\text{H}$ - $^{15}\text{N}$  HSQC spectra of  $^{15}\text{N}$ -labeled KIX (black) and  $^{15}\text{N}$ -labeled KIX plus unlabeled CR3 peptide (red) reveal extensive chemical shift perturbation. b) Overlaid  $^1\text{H}$ - $^{15}\text{N}$  HSQC spectra of KIX (black) and KIX + FCF (domain diagram shown on top) (green) illustrate that the FH domain inhibits the interaction between CR3 and KIX. For panels a and b, the concentration of  $^{15}\text{N}$ -labeled KIX was 0.15 mM, and unlabeled CR3 or FCF was added in a 1:1 molar ratio. c) Pull-down assays were performed using *in vitro* translated Myc-tagged FOXO3a fragments and purified recombinant KIX protein. FOXO3a 151–673 includes the entire FH domain, CR3 domain, and the middle unstructured portion, whereas the N-terminal region of FH is deleted from FOXO3a 244–673. The middle lane in each panel is the negative control with the Ni-resin alone lacking the KIX domain protein.

binding site and the DNA-binding site partially overlap at H3 and the N-terminal loop. The apparent  $K_d$  of CR3–FH interaction determined by NMR titration is

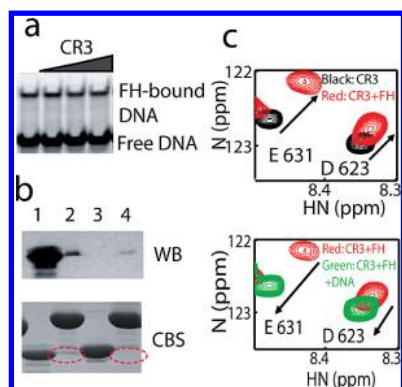


**Figure 4. FRE DNA Disrupts the FOXO3a FH-CR3 Intramolecular Interaction.** a) EMSA shows the FH domain (0.5 ng) binds to the FRE DNA (3.5 ng). With increasing concentration (0–5 ng) of the CR3 peptide, no effect was detected, indicating that CR3 does not compete with DNA binding. b) GST pull-down assays show the addition of FRE DNA decreases the binding of GST-FH to His-Trx-CR3. Two identical gels were run; one was subjected to Western blot (WB) with anti-His tag antibody, and the other was visualized with Coomassie blue stain (CBS). Lanes: 1, input of His-Trx-CR3; 2, His-Trx-CR3 pulled down by GST-FH; 3, control for interaction with GST alone; 4, His-Trx-CR3 pulled down by GST-FH in the presence of FRE DNA. c) The binding of the FH domain (0.25 mM) induces chemical shift changes in the HSQC spectrum of the CR3 domain (0.25 mM), for example, residues D623 and E631 (top panel, from black to red). Addition of the FRE DNA (0.25 mM) to the CR3–FH mixture causes the HSQC peaks of the CR3 domain to move back to the original position of the free state (bottom panel, from red to green) as illustrated for D623 and E631.

about 5  $\mu\text{M}$  (24), and the  $K_d$  of FH–DNA interaction determined by fluorescence anisotropy assay is about 300 nM (28). Thus we examined whether DNA and CR3 compete for FH binding or all three molecules form a ternary complex. We previously demonstrated by electrophoretic mobility shift assay (EMSA) that the recombinant FH domain purified from *E. coli* is capable of binding to the FRE derived from the PUMA promoter (24). Using the same technique, here we found that adding CR3 peptide to the FH–DNA mixture has no effect on the FH–DNA interaction (Figure 4, panel a). However, two experimental methods show that FRE DNA disrupts the intramolecular CR3–FH interaction. Using GST pull-down assays, we demonstrated that the presence of FRE decreases binding of FH to CR3 (Figure 4, panel b). Moreover, whereas addition of unlabeled FH to  $^{15}\text{N}$ -labeled CR3 peptide induced chemical shift changes in the

HSQC peaks of the latter (from black to red Figure 4, panel c), the subsequent addition of FRE DNA to this mixture (DNA to CR3 ratio of 1:1) caused all of the peaks that were perturbed upon FH binding (e.g., E631 and D623) to move back to their original free-state positions (Figure 4, panel c and Supplementary Figure 1, panel c). This observation implies that the FRE DNA oligo effectively displaces CR3 from FH, which may enable CR3 domain to bind to the KIX domain of CBP, recruiting the coactivator to FRE regulated genes. Therefore FH domain binding to the promoter region and the coactivator recruitment may occur simultaneously to initiate transcription in a synergistic manner.

**Mapping the Binding Sites That Mediate the CR3–KIX Interaction.** With the knowledge that the CR3 is released from FH by the FRE DNA to conduct its transactivation function, we employed NMR spectroscopy to obtain structural insight into the CR3–KIX interaction. As it has been shown that the central core region of CR3 mediates the interaction with KIX (Figure 2), we prepared an 18-amino-acid peptide (G618–A635), referred to as CR3 central core (CR3CC) peptide, to characterize the interaction between FOXO3a and its coactivator. The complex of CR3CC with KIX is more soluble under the NMR buffer condition. KIX binding proteins contain a conserved “ $\Phi\text{XX}\Phi\Phi$ ” motif, where “ $\Phi$ ” is a hydrophobic residue, and “X” is an arbitrary residue, of which the most well-studied example is the “LXXLL” motif (38). A sequence alignment of the CR3CC peptide with other KIX-binding transactivation peptides reveals sequence similarity within the “ $\Phi\text{XX}\Phi\Phi$ ” motif. Furthermore CR3CC resembles the c-Myb and c-Jun peptides in the presence of negatively charged residues N-terminal to this motif and at the first “X” position (Figure 5, panel a).

To identify the binding site of the FOXO3a CR3 transactivation domain on KIX,  $^{15}\text{N}$ -labeled KIX domain was titrated with unlabeled CR3CC peptide, and a series of  $^1\text{H}$ – $^{15}\text{N}$  HSQC spectra were recorded with increasing concentration of CR3CC peptide. The titration suggests that the bound and free states are in fast exchange on the NMR chemical shift time scale (Supplementary Figure 2, panel a). As expected, the changes in the KIX HSQC spectrum upon addition of CR3CC peptide resemble those seen upon addition of the whole CR3 domain (Figure 3, panel a and Supplementary Figure 2, panel a), supporting the use of this peptide to study CR3–KIX interaction. The normalized chemical shift change of each backbone resonance was calculated

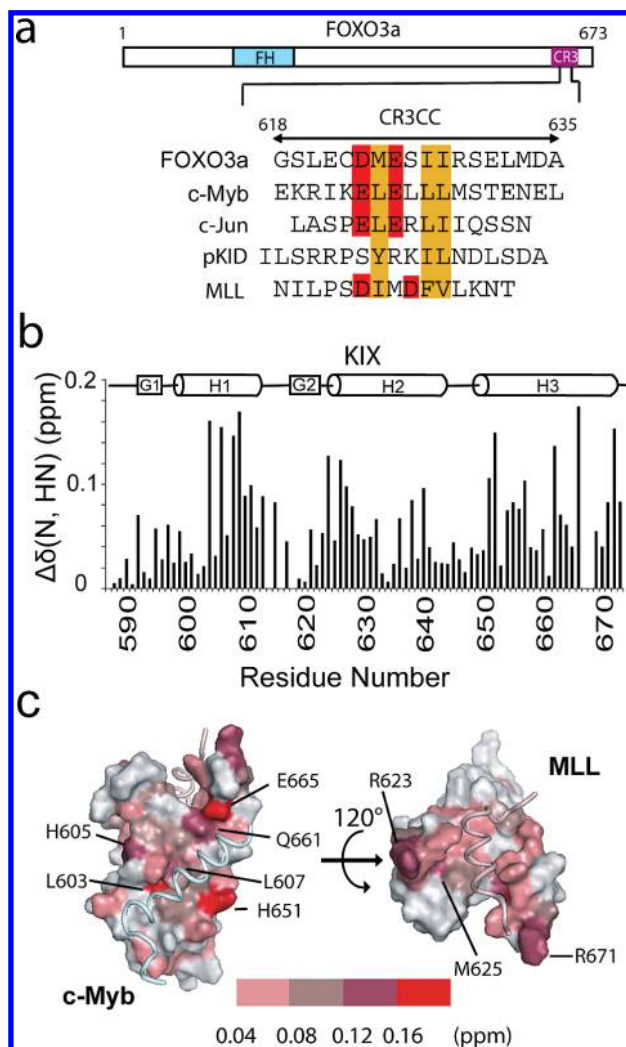


**Figure 5. Mapping the CR3-binding site on KIX by NMR titration.** a) Sequence alignment of CR3CC with other KIX-binding peptides shows high sequence similarity. The conserved hydrophobic residues at the “Φ” position of the “ΦXXΦΦ” motif are highlighted with orange color, and conserved negatively charged residues are highlighted with red color. b) Normalized backbone amide chemical shift changes for  $^{15}\text{N}$ -labeled KIX domain titrated with unlabeled CR3CC peptide were calculated and plotted against residue number of the KIX domain (spectra are shown in Supplementary Figure 2). Secondary structure is indicated on top (cylinder:  $\alpha$  helix, square:  $3_{10}$  helix). c) The residues with large chemical shift perturbation are mapped on the solution structure of the KIX-c-Myb-MLL ternary complex (PDB: 2AGH) and colored according to the magnitude of the normalized chemical shift change. Residues with chemical shift change larger than 0.12 ppm are labeled.

and plotted (Figure 5, panel b), and the residues with large chemical shift changes were identified and mapped on the solution structure of the KIX-c-Myb-MLL ternary complex (PDB: 2AGH) with different colors based the magnitude of normalized chemical shift change (Figure 5, panel c). The KIX fold comprises three  $\alpha$  helices (H1–H3) and two  $3_{10}$  helices (G1 and G2) (Figure 5, panel b) and contains two transactivation peptide-binding hydrophobic grooves. The c-Myb-binding site comprises helices H1 and H3, whereas the MLL binds primarily to a second site on the opposite face formed by H2, H3 together with G2 (36). Binding of CR3CC causes large chemical shift perturbations in regions found near both the c-Myb and MLL-binding sites. The residues L603, H605, L607, H651, Q661, and E665 are clustered in the close vicinity of the c-Myb-binding site, whereas the residues R623, M625, E626, and R671 coincide with the MLL-binding site (Figure 5, panel c). The titration curves of residues from both sites suggest that the CR3CC binds to two sites with similar affinity (Supplementary Figure 2, panel b). Considering that these KIX-interacting transactivation peptides possess high sequence similarity (Figure 5, panel a), it is possible that one peptide can bind to both c-Myb and MLL sites. Indeed, it has been reported that in addition to binding to the c-Myb site, c-Myb and pKID also bind to the MLL site, albeit with lower affinity, and the transactivation (TA) domain of p53 is reported to bind to both sites with similar affinity (34, 39).

#### Determining the Orientation of CR3 Binding by PRE.

Chemical shift perturbation can be caused by binding-induced structural changes as well as the direct interaction. Thus, to confirm that the CR3CC peptide does bind to both c-Myb and MLL-binding sites of KIX and to determine the orientation in which CR3CC peptide binds to these sites, paramagnetic relaxation enhancement (PRE) experiments were employed. The N-terminus of the CR3CC peptide contains a single Cys residue, C622, which can be exploited to attach a spin label without introducing any mutation. An EDTA tag (*N*-[S-(2-pyridylthio)cysteaminy]ethylene-diamine-*N,N,N',N'*-tetraacetic acid) was covalently linked to the cysteine residue and chelated  $\text{Mn}^{2+}$  and  $\text{Ca}^{2+}$  cations were used as the paramagnetic center and the diamagnetic reference, respectively (Figure 6, panel a). Titration of the  $\text{Ca}^{2+}$ -tagged CR3CC peptide into  $^{15}\text{N}$ -labeled KIX induced chemical shift perturbations similar to those seen with the unlabeled peptide, indicating that the EDTA-

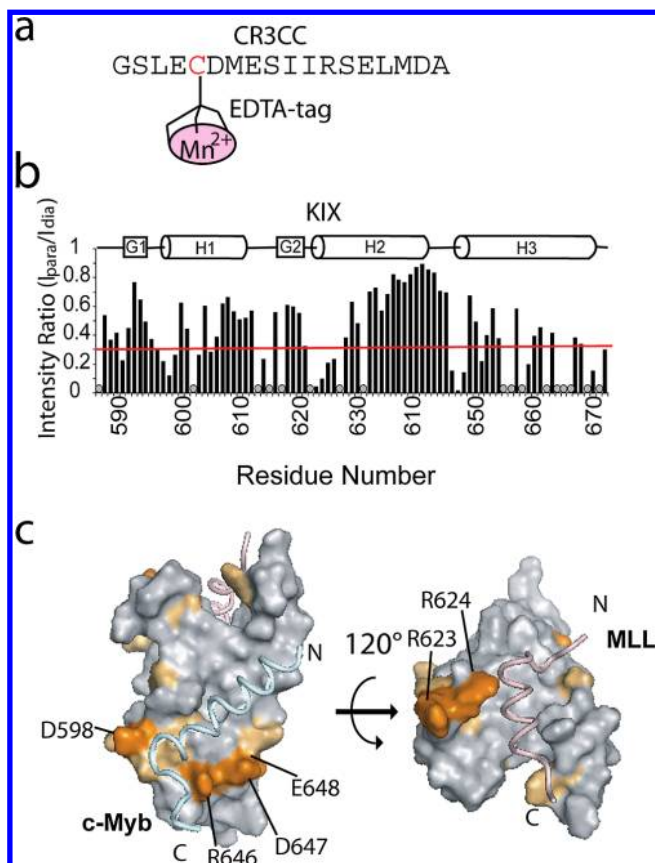


**Figure 6.** Binding site and orientation of CR3 on KIX determined by PRE. **a)** Mn<sup>2+</sup> or Ca<sup>2+</sup> is chelated by a thiol-reactive EDTA tag attached to a lone cysteine residue near the N-terminus of the CR3CC peptide. **b)** The peak intensity ratio of  $I_{para}/I_{dia}$  was calculated and plotted against the residue number of the KIX domain, where  $I_{para}$  is the peak intensity from the KIX with Mn<sup>2+</sup> labeled CR3CC peptide, and  $I_{dia}$  is the peak intensity from the KIX with Ca<sup>2+</sup> labeled CR3CC peptide. The gray dots indicate residues whose peaks are overlapped and thus the intensity cannot be extracted. Residues with a ratio below the red line (0.3) are considered to be significantly broadened as a result of the PRE effect. **c)** Structure of KIX with residues exhibiting an  $I_{para}/I_{dia}$  ratio <0.15 colored orange and labeled, and residues with a ratio <0.3 colored light orange.

cation tag does not affect the CR3-KIX interaction (Supplementary Figures 2, panel a and 3, panel a).

Overlay of the HSQC spectra of KIX in the presence of Mn<sup>2+</sup>- and Ca<sup>2+</sup>-labeled CR3CC peptide show that several specific peaks are broadened by the paramagnetic cation (Supplementary Figure 3, panel b). The peak intensity of each well-resolved backbone amide peak was extracted from the Mn<sup>2+</sup> and Ca<sup>2+</sup> spectra, and the ratio  $I_{para}/I_{dia}$  was plotted (Figure 6, panel b). The residues

for which the backbone amide peak exhibits  $I_{para}/I_{dia} < 0.3$  (under the red line) (Figure 6, panel b) were mapped on the structure of the ternary complex of KIX, c-Myb, and MLL (Figure 6, panel c). Residues from both the c-Myb site and the MLL site are affected by the paramagnetic cation (Figure 6, panel c), strongly supporting our hypothesis that the CR3CC binds to both sites, because the PRE effect only depends on the distance between the atom and the paramagnetic center. Moreover KIX domain residues that are affected dramatically by the Mn<sup>2+</sup> cation with an  $I_{para}/I_{dia} < 0.15$  (orange in Figure 6, panel c) can be used to localize the N-terminus of CR3CC peptide, which contains the modified cysteine residue (Figure 6, panel c). In the c-Myb-binding site, the most broadened peaks are those of D598, R646, D647, and E648, which are clustered at the end of the c-Myb-binding groove, where the C-terminus of c-Myb binds. Thus the CR3CC peptide binds in an orientation opposite that of the c-Myb peptide. Fewer residues are affected at the MLL-binding site; however, two Arg residues, R623 and R624, are severely broadened by binding Mn<sup>2+</sup>-tagged CR3CC peptide. Interactions between KIX and transactivation peptides are determined by both hydrophobic and electrostatic interactions (34). Therefore, these two Arg residues likely become broadened as a result of interaction with the negatively charged CR3 residues (E621 and D623) that flank the tagged C622, and thus the N-terminus of CR3CC is located close to these two Arg when it forms a complex with KIX.

**Conclusions and Significance.** The transcriptional function of FOXO3a includes two processes: sequence-specific DNA recognition and coactivator recruitment, which are conducted by the FH domain and the CR3 domain, respectively. We previously identified an intramolecular interaction between these two domains (24), and here we show that this intramolecular interaction negatively regulates the association of CR3 with KIX (Figure 3 and Figure 7). Moreover, the FRE DNA facilitates the recruitment of CBP by disrupting this in-

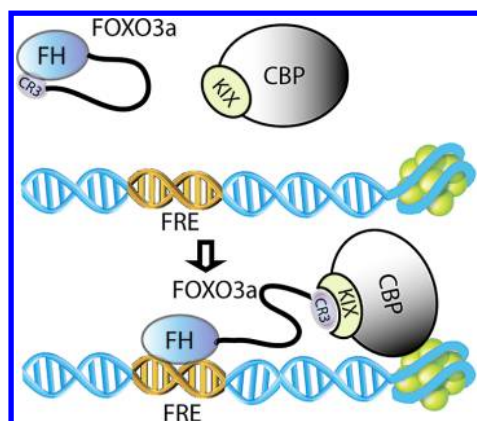


**Figure 7. Model of FOXO3a-dependent coactivator recruitment.** Free FOXO3a is in a closed state with the CR3 domain binding to the FH domain. If the FH domain reaches the FRE DNA in a promoter region, the intramolecular interaction is disrupted upon DNA binding. Then the released CR3 domain interacts with the KIX domain of CBP to initiate the coactivator recruitment. Thus DNA binding and coactivator recruitment occur synergistically.

tramolecular interaction, making CR3 accessible to KIX (Figure 7), which would provide some advantages for its transcriptional function. The transactivation domains of some other eukaryotic transcription factors, including the Zn(II)<sub>2</sub>Cys<sub>6</sub> family members Leu3p and Put3p, are regulated by autoinhibition and only activate transcription after conformational change triggered by binding of a specific metabolite (40, 41). The CR3 domain of FOXO3a is also sequestered by the FH domain until FRE DNA binding activates transcription, which may increase the specificity and selectivity of transactivation. Moreover, the intramolecular interaction would prevent nonproductive protein–protein interactions before transactivation. The “hopping/jumping” model proposes that the DNA-binding protein can be released from nonspecific DNA sequences and diffuse over short distances in solution until it rebinds a nearby location on the same chain, provided it does not interact with other proteins (42, 43). During the diffusion, the CR3 would be sequestered by the FH domain from interaction with other proteins, which may help the FOXO3a molecule rebound to the DNA chain efficiently. After CBP recruitment, sequestration of CR3 by KIX may reciprocally stabilize FH-mediated DNA recognition. Because the FH and CR3 domain are conserved within all mammalian FOXO transcription factors, this mechanism very

likely applies to other FOXO proteins. FOXO3a is controlled by many signaling pathways (4, 16), so this transactivation mechanism may be further regulated by other proteins through many post-translational modification sites in the IDRs according to diverse stimuli.

The interaction between FOXO3a CR3 transactivation domain and the KIX domain of CBP appears to involve multiple binding sites. Our data suggest that the core region of the CR3 domain could bind to the KIX domain at two distinct sites. It is possible that the short peptide utilized in our NMR studies may behave differently than the full length FOXO3a protein *in vivo*; however, many previous results are consistent with our observation. It has been reported that two sites on KIX can be occupied by transactivation domains of two different proteins (*e.g.*, c-Myb and MLL) in a synergistic manner, by two copies of the same transactivation domain (*e.g.*, c-Myb or pKID), or by two distinct parts of one transactivation domain (*e.g.*, p53 AD1 and AD2) (34–36, 39). Like AD1 and AD2 motifs of p53 TA domain, the FOXO3a CR3 domain binds to two sites (34), and interestingly, the binding orientation of CR3 in the c-Myb-binding site is different from that of the c-Myb peptide by about 180°, revealing new structural features of transactivation domain recognition by KIX. The propensity of CR3 to form a helical structure has been examined by TFE titration experiments (24), and our chemical shift index (CSI) data also show that the CR3CC peptide undergoes binding-induced folding into a helical structure upon interaction with the KIX domain (Supplementary Figure 4). Abrogation of the interaction between CR3 and KIX by deletion of the CR3 domain diminishes transactivation activity in luciferase assays, and these studies also suggest that full transactivation activity of FOXO3a also requires another region, the CR2 domain, which contains an “LXXLL” motif (14, 31). We have demonstrated that a peptide derived from CR2 including the “LXXLL” motif also binds to KIX (unpublished data). It appears that both CR2 and CR3 bind to the KIX domain to recruit coactivator CBP, yet the exact role of the CR2 region is currently unknown. In addition to this, the promoter region of FOXO-regulated genes usually contains multiple copies of FRE. As a consequence, in the cell, more than one FOXO3a molecule may interact with CBP at the same time through different regions, potentially enhancing the efficiency of the FOXO3a-dependent coactivator recruitment.

This work sheds light on the regulatory role of the FH–CR3 interaction in promoter binding and coactivator recruitment, which can occur synergistically as evidenced by our NMR studies. Furthermore, our data on CR3–KIX interaction shows a promiscuous binding of CR3 to two hydrophobic grooves on KIX in a manner analogous to the p53–KIX interaction reported by Wright and co-workers

(34). These studies provide insight into FOXO3a-dependent transcriptional activation mechanisms, which are likely conserved throughout the FOXO protein subfamily on the basis of the high sequence similarity. Our challenge is to demonstrate this conformational change-coupled FOXO3a–CBP/p300 interplay in *in vivo* transcription, which will be addressed in future studies.

## METHODS

**Sample Preparation.** FOXO3a FH domain (S151–A251), CR3 domain (D610–N650), the FCF protein (FH-(GS)<sub>4</sub>-CR3), His-Trx-CR3, and Myc-tagged FOXO3a fragments (S151–G673 and G244–G673) were constructed, expressed, and purified as previously described (24). The KIX domain of mouse CBP (G586–L672) in pET21a vector was a gift from Dr. Peter E. Wright, and its sequence is identical to human KIX. The KIX domain was expressed and purified using the same method as described (33).

The CR3 central core region (CR3CC) was obtained by annealing two single-stranded DNA oligos (Sigma Genosys) and cloned into pGEX4T-1 vector (GE Healthcare) using *Bam*HI and *Xho*I sites. CR3CC was expressed in *E. coli* BL21 (DE3) cells by induction with 0.6 mM isopropyl- $\beta$ -D-thiogalactoside (IPTG) at 37 °C for 3 h. For labeled proteins, culture was prepared in M9 media supplemented with <sup>15</sup>N ammonium chloride and/or <sup>13</sup>C glucose. The cells were harvested by centrifugation and lysed by sonication. GST-fusion CR3CC was purified by Glutathione Sepharose 4B (GE Healthcare) and cut from the resin by thrombin at RT overnight. The CR3CC peptide after thrombin cleavage has the sequence of G618–A635. Cleaved peptide was further purified on a Superdex peptide 10/300 GL (GE Healthcare) column. The purity was checked by mass-spectrometry and the purified peptide was dialyzed into water and lyophilized for stock.

The cy5-labeled FRE DNA constructs (5'-GTTTGTTTACAAA-CAATG-3'; 5'-CATTGTTTGTAAACAAAC-3') for EMSA and the unlabeled DNA constructs (5'-GCACAACAACG-3', and 5'-CGTTGTTGTGC-3') for NMR and pull-down derived from the PUMA promoter were prepared as HPLC-purified single-stranded oligos (Sigma Genosys). The double-stranded DNA was obtained by annealing two single-stranded DNA constructs.

**Pull-Down Assays.** The purified KIX domain protein was re-bound to the Ni-charged resin (Bio-RAD) as the bait. The *in vitro* translated Myc-tagged FOXO3a fragments bound with His-KIX and Ni-resin for 1 h at 4 °C. After washing the beads 3 times with the washing buffer (20 mM Hepes-NaOH, pH 7.9, 10% glycerol, 0.5 M KCl, 1 mM DTT, and 0.1% NP-40), the proteins retained on the beads were extracted in 25  $\mu$ L of SDS–PAGE sample buffer and were separated on SDS–PAGE. Proteins were detected by Western blotting with a mouse monoclonal anti-Myc antibody (Cell Signaling Technology). Purified His-Trx-CR3 and immobilized GST-FH proteins were used for GST pull-down assays. His-Trx-CR3 bound with GST-FH (in presence and absence of FRE DNA) and with GST for 1 h at 4 °C. After washing the beads with 30 column volumes of washing buffer (PBS + 0.1% NP-40), the proteins retained on the beads were extracted and separated on SDS–PAGE. The antipenta-His (Qiagen) was used in Western blot analysis.

**Electrophoretic Mobility Shift Assays (EMSA).** The buffer, reaction conditions, and method of visualization are the same as previously described (24). The sample for each lane contains 3.5 ng DNA, 0.5 ng FH protein, and a gradient of the CR3 protein was applied to each sample as 0, 0.1, 0.5, and 5 ng.

**NMR Spectroscopy.** Two-dimensional <sup>1</sup>H–<sup>15</sup>N heteronuclear single quantum coherence (HSQC) spectra (44) and three-dimensional triple-resonance spectra HNCACB (45), and CBCA–CONNH (46) were collected for the backbone chemical shift assignments and NMR-based chemical shift perturbation and competition assays for the KIX and CR3CC. The spectra were processed and visualized by NMRPipe (47) and NMRView (48), and resonance assignments were made using XEASY (49). NMR spectra with the CR3CC peptide present were recorded at 30 °C, whereas others were recorded at 25 °C, and the Bruker 800-MHz AVANCE II spectrometer with TCI cryoprobe was used for data collection. The DNA competition assays were performed in 20 mM NaPi, pH = 6.5, 50 mM KCl, 2 mM DTT, 10% D<sub>2</sub>O, and 0.5 mM NaN<sub>3</sub>. The buffer for all other NMR samples is 20 mM MES pH = 6.0, 100 mM NaCl, 2 mM DTT, 8% D<sub>2</sub>O, and 0.5 mM NaN<sub>3</sub> (DTT was removed for the buffer of paramagnetic relaxation enhancement experiments).

The method of paramagnetic relaxation enhancement (PRE) experiments was modified from ref 50. A single cysteine residue close to the N-terminus in the native sequence of the CR3CC peptide was used for EDTA-labeling. The CR3CC peptide powder was dissolved in NMR buffer plus 5 mM DTT, and then DTT was removed by desalting column PD Miditrap G-25 (GE Healthcare). A 5-fold excess of *N*-[5-(2-pyridylthio)cysteaminy] ethylene-diamine-*N,N,N',N'*-tetraacetic acid (Toronto Research Chemicals) and 10-fold excess of divalent cation (Mn<sup>2+</sup> or Ca<sup>2+</sup>) were quickly added into the CR3CC peptide solution and incubated at RT overnight. The excess free EDTA tag and cations were removed using a desalting column. The Mn<sup>2+</sup> (paramagnetic cation) or Ca<sup>2+</sup> (diamagnetic cation) labeled CR3CC peptides were added into the <sup>15</sup>N-labeled KIX respectively with roughly 1:2 ratio. The HSQC spectra were recorded for each sample, intensity ratios of well-resolved HSQC peaks were extracted using XEASY, and  $I_{para}/I_{dia}$  were calculated, where  $I_{para}$  is the resonance intensity of the sample with Mn<sup>2+</sup>-labeled CR3CC peptide and  $I_{dia}$  is the resonance intensity of the sample with Ca<sup>2+</sup>-labeled CR3CC peptide.

**Acknowledgment:** We thank Dr. P. Wright for the KIX expression vector and helpful discussion. This work is supported by the Canadian Institutes of Health Research (CIHR) to M.I.; C.B.M. holds a CIHR postdoctoral fellowship. Canadian Foundation of Innovation provided an 800 MHz NMR spectrometer at the Toronto Medical Discovery Tower. M.I. holds a Canada Research Chair in Cancer Structural Biology.

**Supporting Information Available:** This material is available free of charge via the Internet at <http://pubs.acs.org>.

## REFERENCES

1. Kaestner, K. H., Knochel, W., and Martinez, D. E. (2000) Unified nomenclature for the winged helix/forkhead transcription factors, *Genes Dev.* 14, 142–146.

2. Clark, K. L., Halay, E. D., Lai, E., and Burley, S. K. (1993) Co-crystal structure of the HNF-3/fork head DNA-recognition motif resembles histone H5, *Nature* **364**, 412–420.
3. Kaufmann, E., and Knöchel, W. (1996) Five years on the wings of fork head, *Mech. Dev.* **57**, 3–20.
4. Arden, K. C., and Biggs, W. H., 3rd. (2002) Regulation of the FoxO family of transcription factors by phosphatidylinositol-3 kinase-activated signaling, *Arch. Biochem. Biophys.* **403**, 292–298.
5. Greer, E. L., and Brunet, A. (2005) FOXO transcription factors at the interface between longevity and tumor suppression, *Oncogene* **24**, 7410–7425.
6. Borkhardt, A., Repp, R., Haas, O. A., Leis, T., Harbott, J., Kreuder, J., Henn, T., and Lampert, F. (1997) Cloning and characterization of AFX, the gene that fuses to MLL in acute leukemias with a t(X;11)(q13;q23), *Oncogene* **14**, 195–202.
7. Anderson, M. J., Viars, C. S., Czekay, S., Cavenee, W. K., and Arden, K. C. (1998) Cloning and characterization of three human Forkhead genes that comprise an FKHR-like gene subfamily, *Genomics* **47**, 187–199.
8. Arden, K. C. (2008) FOXO animal models reveal a variety of diverse roles for FOXO transcription factors, *Oncogene* **27**, 2345–2350.
9. Jacobs, F. M., van der Heide, L. P., Wijchers, P. J., Burbach, J. P., Hoekman, M. F., and Smidt, M. P. (2003) FoxO6, a novel member of the FoxO class of transcription factors with distinct shuttling dynamics, *J. Biol. Chem.* **278**, 35959–35967.
10. Pierrou, S., Hellqvist, M., Samuelsson, L., Enerbäck, S., and Carlsson, P. (1994) Cloning and characterization of seven human forkhead proteins: binding site specificity and DNA bending, *EMBO J.* **13**, 5002–5012.
11. Jonsson, H., and Peng, S. L. (2005) Forkhead transcription factors in immunology, *Cell. Mol. Life Sci.* **62**, 397–409.
12. Spiegelman, B. M., and Heinrich, R. (2004) Biological control through regulated transcriptional coactivators, *Cell* **119**, 157–167.
13. Nasrin, N., Ogg, S., Cahill, C. M., Biggs, W., Nui, S., Dore, J., Calvo, D., Shi, Y., Ruvkun, G., and Alexander-Bridges, M. C. (2000) DAF-16 recruits the CREB-binding protein coactivator complex to the insulin-like growth factor binding protein 1 promoter in HepG2 cells, *Proc. Natl. Acad. Sci. U.S.A.* **97**, 10412–10417.
14. So, C. W., and Cleary, M. L. (2002) MLL-AFX requires the transcriptional effector domains of AFX to transform myeloid progenitors and transdominantly interfere with forkhead protein function, *Mol. Cell. Biol.* **22**, 6542–6552.
15. Accili, D., and Arden, K. C. (2006) FoxOs at the crossroads of cellular metabolism, differentiation, and transformation, *Cell* **117**, 421–426.
16. Barthel, A., Schmoll, D., and Unterman, T. G. (2005) FoxO proteins in insulin action and metabolism, *Trends Endocrinol. Metab.* **16**, 183–189.
17. Birkenkamp, K. U., and Coffey, P. J. (2003) Regulation of cell survival and proliferation by the FOXO (Forkhead box, class O) subfamily of Forkhead transcription factors, *Biochem. Soc. Trans.* **31**, 292–297.
18. Lynch, R. L., Konicek, B. W., McNulty, A. M., Hanna, K. R., Lewis, J. E., Neubauer, B. L., and Graff, J. R. (2005) The progression of LNCaP human prostate cancer cells to androgen independence involves decreased FOXO3a expression and reduced p27KIP1 promoter transactivation, *Mol. Cancer Res.* **3**, 163–169.
19. Tran, H., Brunet, A., Grenier, J. M., Datta, S. R., Jr, DiStefano, P. S., Chiang, L. W., and Greenberg, M. E. (2002) DNA repair pathway stimulated by the forkhead transcription factor FOXO3a through the Gadd45 protein, *Science* **296**, 530–534.
20. Yang, L., Xie, S., Jamaluddin, M. S., Altuwajri, S., Ni, J., Kim, E., Chen, Y. T., Hu, Y. C., Wang, L., Chuang, K. H., Wu, C. T., and Chang, C. (2005) Induction of androgen receptor expression by phosphatidylinositol 3-Kinase/Akt downstream substrate, FOXO3a, and their roles in apoptosis of LNCaP prostate cancer cells, *J. Biol. Chem.* **280**, 33558–33565.
21. You, H., Pellegrini, M., Tsuchihara, K., Yamamoto, K., Hacker, G., Erlacher, M., Villunger, A., and Mak, T. W. (2006) FOXO3a-dependent regulation of Puma in response to cytokine/growth factor withdrawal, *J. Exp. Med.* **203**, 1657–1663.
22. Gilley, J., Coffey, P. J., and Ham, J. (2003) FOXO transcription factors directly activate bim gene expression and promote apoptosis in sympathetic neurons, *J. Cell Biol.* **162**, 613–622.
23. You, H., Yamamoto, K., and Mak, T. W. (2006) Regulation of transactivation-independent proapoptotic activity of p53 by FOXO3a, *Proc. Natl. Acad. Sci. U.S.A.* **103**, 9051–9056.
24. Wang, F., Marshall, C. B., Yamamoto, K., Li, G. Y., Plevin, M. J., You, H., Mak, T. W., and Ikura, M. (2008) Biochemical and structural characterization of an intramolecular interaction in FOXO3a and its binding with p53, *J. Mol. Biol.* **384**, 590–603.
25. Tsai, W. B., Chung, Y. M., Takahashi, Y., Xu, Z., and Hu, M. C. (2008) Functional interaction between FOXO3a and ATM regulates DNA damage response, *Nat. Cell Biol.* **10**, 460–467.
26. Hoogeboom, D., Essers, M. A., Polderman, P. E., Voets, E., Smits, L. M., and Burgering, B. M. (2008) Interaction of FOXO with beta-catenin inhibits beta-catenin/T cell factor activity, *J. Biol. Chem.* **283**, 9224–9230.
27. Weigelt, J., Climent, I., Dahlman-Wright, K., and Wikström, M. (2001) Solution structure of the DNA binding domain of the human forkhead transcription factor AFX (FOXO4), *Biochemistry* **40**, 5861–5869.
28. Tsai, K. L., Sun, Y. J., Huang, C. Y., Yang, J. Y., Hung, M. C., and Hsiao, C. D. (2007) Crystal structure of the human FOXO3a-DBD/DNA complex suggests the effects of post-translational modification, *Nucleic Acids Res.* **35**, 6984–6994.
29. Brent, M. M., Anand, R., and Marmorstein, R. (2008) Structural basis for DNA recognition by FoxO1 and its regulation by posttranslational modification, *Structure* **16**, 1407–1416.
30. Bryson, K., McGuffin, L. J., Marsden, R. L., Ward, J. J., Sodhi, J. S., and Jones, D. T. (2005) Protein structure prediction servers at University College London, *Nucleic Acids Res.* **33**, W36–W38.
31. So, C. W., and Cleary, M. L. (2003) Common mechanism for oncogenic activation of MLL by forkhead family proteins, *Blood* **101**, 633–639.
32. Radhakrishnan, I., Pérez-Alvarado, G. C., Parker, D., Dyson, H. J., Montminy, M. R., and Wright, P. E. (1997) Solution structure of the KIX domain of CBP bound to the transactivation domain of CREB: a model for activator:coactivator interactions, *Cell* **91**, 741–752.
33. Zor, T., Mayr, B. M., Dyson, H. J., Montminy, M. R., and Wright, P. E. (2002) Roles of phosphorylation and helix propensity in the binding of the KIX domain of CREB-binding protein by constitutive (c-Myb) and inducible (CREB) activators, *J. Biol. Chem.* **277**, 42241–42248.
34. Lee, C. W., Arai, M., Martinez-Yamout, M. A., Dyson, H. J., and Wright, P. E. (2009) Mapping the interactions of the p53 transactivation domain with the KIX domain of CBP, *Biochemistry* **48**, 2115–2124.
35. Goto, N. K., Zor, T., Martinez-Yamout, M., Dyson, H. J., and Wright, P. E. (2002) Cooperativity in transcription factor binding to the coactivator CREB-binding protein (CBP). The mixed lineage leukemia protein (MLL) activation domain binds to an allosteric site on the KIX domain, *J. Biol. Chem.* **277**, 43168–43174.
36. De Guzman, R. N., Goto, N. K., Dyson, H. J., and Wright, P. E. (2006) Structural basis for cooperative transcription factor binding to the CBP coactivator, *J. Mol. Biol.* **355**, 1005–1013.
37. Boura, E., Silhan, J., Herman, P., Vecer, J., Sulc, M., Teisinger, J., Obsilova, V., and Obsil, T. (2007) Both the N-terminal loop and wing W2 of the forkhead domain of transcription factor Foxo4 are important for DNA binding, *J. Biol. Chem.* **282**, 8265–8275.
38. Plevin, M. J., Mills, M. M., and Ikura, M. (2005) The LxxLL motif: a multifunctional binding sequence in transcriptional regulation, *Trends Biochem. Sci.* **30**, 66–69.

39. Sugase, K., Dyson, H. J., and Wright, P. E. (2007) Mechanism of coupled folding and binding of an intrinsically disordered protein, *Nature* **447**, 1021–1025.
40. Sze, J. Y., Woontner, W., Jaehning, J. A., and Kohlhaw, G. B. (1992) *In vitro* transcriptional activation by a metabolic intermediate: activation by Leu3 depends on alpha-isopropylmalate, *Science* **258**, 1143–1145.
41. Sellick, C. A., and Reece, R. J. (2003) Modulation of transcription factor function by an amino acid: activation of Put3p by proline, *EMBO J.* **22**, 5147–5153.
42. Widom, J. (2005) Target site localization by site-specific, DNA-binding proteins, *Proc. Natl. Acad. Sci. U.S.A.* **102**, 16909–16910.
43. Gowers, D. M., Wilson, G. G., and Halford, S. E. (2005) Measurement of the contributions of 1D and 3D pathways to the translocation of a protein along DNA, *Proc. Natl. Acad. Sci. U.S.A.* **102**, 15883–15888.
44. Bodenhausen, G., and Ruben, D. (1980) Natural abundance  $^{15}\text{N}$  NMR by enhanced heteronuclear spectroscopy, *Chem. Phys. Lett.* **69**, 185–189.
45. Wittekind, M., and Mueller, L. (1993) HNCACB, a high-sensitivity 3D NMR experiment to correlate amide-proton and nitrogen resonances with the alpha- and beta-carbon resonances in proteins, *J. Magn. Reson.* **101**, 201–205.
46. Grzesiek, S., and Bax, A. (1992) Improved 3D triple-resonance NMR techniques applied to a 31 kDa protein, *J. Magn. Reson.* **96**, 432–440.
47. Delaglio, F., Grzesiek, S., Vuister, G. W., Zhu, G., Pfeifer, J., and Bax, A. (1995) NMRPipe: a multidimensional spectral processing system based on UNIX pipes, *J. Biomol. NMR* **6**, 277–293.
48. Johnson, B. A. (2004) Using NMRView to visualize and analyze the NMR spectra of macromolecules, *Methods Mol. Biol.* **278**, 313–352.
49. Bartels, C., Xia, T., Billeter, M., Guntert, P., and Wuthrich, K. (1995) The program XEASY for computer-supported NMR spectral analysis of biological macromolecules, *J. Biomol. NMR* **6**, 1–10.
50. Tang, C., Iwahara, J., and Clore, G. M. (2006) Visualization of transient encounter complexes in protein-protein association, *Nature* **444**, 383–386.
51. DeLano, W. L. (2002) *The PyMOL Molecular Graphics System*, DeLANO Scientific, Palo Alto, CA.